In Vivo Calcium Accumulation in Presynaptic and Postsynaptic Dendrites of Visual Interneurons

VOLKER DÜRR[1,2] AND MARTIN EGELHAAF[1,2]

[1]*Lehrstuhl für Neurobiologie, Fakultät für Biologie, Universität Bielefeld, D-33501 Bielefeld, Germany; and* [2]*Centre for Visual Sciences, Research School for Biological Sciences, Australian National University, Canberra, ACT 2600, Australia*

Dürr, Volker and Martin Egelhaaf. In vivo calcium accumulation in presynaptic and postsynaptic dendrites of visual interneurons. *J. Neurophysiol.* 82: 3327–3338, 1999. In this comparative in vivo study of dendritic calcium accumulation, we describe the time course and spatial integration properties of two classes of visual interneurons in the lobula plate of the blowfly. Calcium accumulation was measured during visual motion stimulation, ensuring synaptic activation of the neurons within their natural spatial and temporal operating range. The compared cell classes, centrifugal horizontal (CH) and horizontal system (HS) cells, are known to receive retinotopic input of similar direction selectivity, but to differ in morphology, biophysics, presence of dendrodendritic synapses, and computational task. *1)* The time course of motion-induced calcium accumulation was highly invariant with respect to stimulus parameters such as pattern contrast and size. In HS cells, the rise of $[Ca^{2+}]_i$ can be described by a single exponential with a time constant of 5–6 s. The initial rise of $[Ca^{2+}]_i$ in CH cells was much faster ($\tau \approx 1$ s). The decay time constant in both cell classes was estimated to be at least 3.5 times longer than the corresponding rise time constant. *2)* The voltage-$[Ca^{2+}]_i$ relationship was best described by an expansive nonlinearity in HS cells and an approximately linear relationship in CH cells. *3)* Both cell classes displayed a size-dependent saturation nonlinearity of the calcium accumulation. Although in CH cells calcium saturation was indistinguishable from saturation of the membrane potential, saturation of the two response parameters differed in HS cells. *4)* There was spatial overlap of the calcium signal in response to nonoverlapping visual stimuli. Both the area and the amplitude of the overlap profile was larger in CH cells than in HS cells. Thus calcium accumulation in CH cells is spatially blurred to a greater extent than in HS cells. *5)* The described differences between the two cell classes may reflect the following computational tasks of these neurons: CH cells relay retinotopic information within the lobula plate via dendritic synapses with pronounced spatial low-pass filtering. HS cells are output neurons of the lobula plate, in which the slow, local calcium accumulation may be suitable for local modulatory functions.

INTRODUCTION

A central question about the computational function of sensory interneurons is how the integrative properties of their dendrites shape the overall tuning characteristics to certain features of the stimulus (Borst and Egelhaaf 1994). Because the dendrite represents the input zone of the neuron, visualizing the spatiotemporal activity patterns, as was done here by monitoring the intracellular concentration of ionic free calcium $[Ca^{2+}]_i$, can be expected to yield important clues about the computations performed by the respective neuron.

The functional significance of $[Ca^{2+}]_i$ in invertebrate neurons is manifold (Kostyuk 1992), comprising essential mechanisms such as transmitter release (Katz 1969), synaptic plasticity (Denk et al. 1996; Regehr and Tank 1994), triggering or modulation of biochemical and genetic signaling pathways (Ghosh and Greenberg 1995), modulatory actions on ion channels in the outer cell membrane (Sah 1996), and intracellular stores (Berridge 1997; Hardie 1996), as well as charge transfer, leading to depolarization of the cell membrane (Skeer et al. 1996).

Although calcium imaging has become a standard technique in neurophysiology, in vivo studies of dendritic $[Ca^{2+}]_i$ dynamics have mainly been restricted to insect sensory systems (Borst and Egelhaaf 1992; Egelhaaf and Borst 1995; Egelhaaf et al. 1993; Ogawa et al. 1996; Single and Borst 1998; Sobel and Tank 1992; but see Svoboda et al. 1997). The lobula plate of the fly remains one of the few model systems, where dendritic calcium accumulation can be studied in vivo in individually identifiable neurons, the biophysical properties as well as the behavioral context of which are known. In taking advantage of this detailed knowledge, the present comparative study focuses on distinct differences in dendritic calcium accumulation between two neuron classes, the centrifugal horizontal (CH) and horizontal system (HS) cells, both of which receive similar retinotopic input but drastically differ in their functional properties. While CH cells are relay neurons within the lobula plate, bearing presynaptic specializations across their entire dendritic arborization (Gauck et al. 1997), HS cells are output elements of the lobula plate, possessing purely postsynaptic dendrites (Hausen et al. 1980). The comparison of calcium accumulation in CH and HS cells therefore promises new insights into the general characteristics of information processing at dendritic synapses such as the kinetics of calcium-mediated mechanisms and the spatial scale of interactions within an array of dendritic synapses.

The lobula plate is a layered neuropile in the optic lobe, containing the dendrites of a set of motion-sensitive, large-field visual interneurons, the tangential cells. Among them, ~30 have been identified and characterized in some detail (e.g., Douglass and Strausfeld 1996; Eckert and Dvorak 1983; Egelhaaf 1985; Hausen 1976, 1981, 1982a,b, 1984). All of these are directionally selective to visual motion and have been discussed in the behavioral context of gaze stabilization, course control and figure-ground discrimination (reviews: Egelhaaf and Borst 1993; Hausen and Egelhaaf 1989).

In CH and HS cells, visual stimulation of the ipsilateral part of their receptive field leads to graded depolarization of the

The costs of publication of this article were defrayed in part by the payment of page charges. The article must therefore be hereby marked "*advertisement*" in accordance with 18 U.S.C. Section 1734 solely to indicate this fact.

membrane potential during front-to-back horizontal motion, and graded hyperpolarization during motion in the opposite direction. This ipsilateral input is mediated to the lobula plate arborization by a large array of retinotopically organized inhibitory and excitatory local elements. Previous optical imaging studies have demonstrated that dendritic calcium accumulation in HS cells is fast and sustained, occurring within a few hundred milliseconds after onset of visual motion, with increasing $[Ca^{2+}]_i$ over stimulus periods up to 30 s (Egelhaaf and Borst 1995). The same study also showed that $[Ca^{2+}]_i$ in HS cells was significantly raised in response to stimulus motion in the preferred direction of the cells but remained virtually unchanged in response to motion in the opposite direction (null direction). This finding also indicated the presence of a voltage-dependent calcium influx, because the activation of cholinergic, ligand-gated currents is thought to be only weakly direction selective (Borst et al. 1995; Single et al. 1997). Voltage-dependent calcium influx has also been confirmed by DC injection into the dendrites of various tangential cells (Egelhaaf and Borst 1995; Single and Borst 1997, 1998).

CH cells

The class of CH cells comprises two cells in each half of the brain, one with an arborization within the dorsal part of the lobula plate (DCH), the other with an arborization in the ventral part (VCH) (Eckert and Dvorak 1983; Hausen 1976). Both CH cells are inhibitory, GABAergic neurons (Meyer et al. 1986; Strausfeld et al. 1995).

In a recent electron-microscopical study of the VCH cell, Gauck et al. (1997) describe postsynaptic specializations in both the main arborization in the lobula plate and a second, smaller arborization that is located in the protocerebrum. The only presynaptic specializations of VCH are synaptic connections between the dendrite of VCH and other unidentified neurites within the lobula plate (Gauck et al. 1997). Gauck et al. also describe one finding of reciprocal synapses in this region. In spite of the lack of detailed anatomic studies of DCH, light-microscopical and electrophysiological characteristics of DCH suggest similar dendritic synapses in both CH cells. In the context of dendritic calcium accumulation, this is particularly interesting because the two-dimensional distribution of $[Ca^{2+}]_i$ is likely to reflect the distribution of presynaptic activity throughout the array of dendritic chemical synapses. Because Gauck et al. have found pre- and postsynaptic specializations within a range of 0.1 μm, the presynaptic activity pattern is expected to be relayed into a very similar postsynaptic activity pattern of reversed sign.

The dendritic inhibition mediated by VCH has been discussed in the functional context of figure-ground discrimination, based on a laser ablation study (Warzecha et al. 1993), optical imaging results (Egelhaaf et al. 1993), and modeling approaches (Borst and Egelhaaf 1993).

HS cells

The class of HS cells comprises a set of three neurons in each half of the brain (Hausen 1976, 1982a,b). The dendritic arborizations of HS cells are exclusively located in the lobula plate, and their receptive fields are juxtaposed in a dorsoventral order relative to the visual equator (north: HSN; equatorial: HSE; south: HSS). Their dendrites bear input specializations on spinelike protrusions of their main branches as well as on second and higher order branches (Hausen et al. 1980). The graded depolarizations have superimposed on them spikelike depolarizations, which disappear after treatment with tetrodotoxin and therefore are thought to be caused by a voltage-activated Na current (Haag et al. 1997) rendering the dendrite a fast response element to oscillatory stimulation (Haag and Borst 1996).

HS cells make synaptic output connections only in the terminal region located in the protocerebrum (Hausen et al. 1980). In contrast to CH cells, the transmitter of HS cells is unknown.

In a functional context, HS cells have been discussed as part of the neural substrate mediating optomotor responses around the vertical axis of the animal. This interpretation is supported by experiments with the *Drosophila* mutant "optomotor blind," which lacks both HS and VS cells (Heisenberg et al. 1978), by lesion experiments using laser ablation of individual cells (Geiger and Nässel 1981, 1982) and microsurgical severing of certain fiber tracts (Hausen and Wehrhahn 1990) and by the overall similarities of the electrical response properties and the turning behavior of flying blowflies (Hausen and Wehrhahn 1989).

Although the identity of the presynaptic neurons of CH and HS cells is still unknown, their receptive fields, directional tuning properties, and region of arborization indicate that the ipsilateral input of CH and HS cells can be assumed to be very alike. Yet their output organization and membrane properties reveal fundamental differences. The present study will show that calcium accumulation in these cell classes differs considerably, manifesting the functional tasks of these neurons.

A preliminary account of this study has been published in abstract form (Dürr and Egelhaaf 1997).

METHODS

Animal preparation

Experiments were carried out on 1- to 3-day-old female blowflies of the genus *Calliphora* (*C. erythrocephala* in Bielefeld, Germany and *C. stygia* in Canberra, Australia). *C. erythrocephala* was taken from laboratory stock, bred at the University of Bielefeld. *C. stygia* pupae were supplied by the CSIRO Division of Entomology in Canberra. Generally, electrophysiological responses and calcium signals in the lobula plate neurons of both species were indistinguishable. Also, the overall morphology of the neurons was the same in both species, although *C. stygia* neurons were larger than *C. erythrocephala* neurons. Minor anatomic differences such as the slightly more distal location of the soma in VS cells of *C. stygia* did not contradict pooling of data from both species. Still, separate treatment of the experimental results obtained from the two species was necessary where exact matching of the stimulus parameters was required, e.g., in measurements of contrast dependency of calcium accumulation. Unless explicitly stated for particular figures and data sets, all results presented were acquired on *C. erythrocephala*. The animals were anesthetized with carbon dioxide, and the thorax was waxed to a glass support. Then the legs were removed and the wings and abdomen were immobilized with wax. The head was pitched downward, and the genae were waxed to the thorax. Subsequently, a hole was cut into the back of the head, such that the brain was accessible and the right lobula plate was visible from above. Neck muscles were severed, and antennae, haustellum, gut, fat body and heart were removed. The abdomen was filled with Ringer solution (concentrations in mM:

128.3 NaCl, 5.4 KCl, 1.9 $CaCl_2$, 4.8 $NaHCO_3$, 3.3 Na_2HPO_4, 3.4 KH_2PO_4, 13.9 glucose, pH 7.0; all chemicals from Merck), and all wounds were sealed with wax. Finally the main tracheae running across the optic lobes were plugged.

Stimulus procedure

The fly was mounted under an epifluorescence microscope (Zeiss Universal III-RS) with its head facing downward into an opaque sphere (∅ 36 mm). Two stripe patterns (∅ 66°) could be projected onto this sphere from below. The spatial wavelength of the stimulus pattern amounted to ~33° (with local distortions due to the projection), and the contrast was 0.68 (except for experiments on contrast dependency) at a mean light intensity of 230 cd/m^2. The spectrum of the stimulus light was that of a Hg-arc-lamp (Osram HBO 100 W). Note that these measures only give a lower estimate of the physiologically relevant light intensity to a fly, because Hg-arc lamps emit blue and ultraviolet (UV) light at high intensities, which excite Dipteran photoreceptors considerably (Hardie 1982), while this spectral range is largely neglected in the usual photometric measures as obtained from a luminance meter (Minolta). Both stripe patterns could be shifted along the horizontal and vertical axis as seen from the fly, and each of them could be occluded separately (single-field stimulus). Furthermore, they could be rotated independently by means of dove prisms, such that the orientation of the pattern could be adjusted to the preferred direction of the recorded visual interneuron. The temporal frequency of the moving pattern was always set to 2 Hz, corresponding to a pattern velocity of ~66°/s. The location of the two visual stimulus fields was adjusted individually for each electrophysiological recording, such that motion in either field elicited significant change in membrane potential. The stimulus fields covered the ipsilateral frontal region of the receptive field of the recorded neuron. Stimulation of the contralateral eye was prevented by shifting the stimuli such that the characteristic electrical response components for contralateral stimulation disappeared [excitatory postsynaptic potentials (EPSPs) and inhibitory postsynaptic potentials (IPSPs) in CH cells, EPSPs in HSE and HSN]. Precision of stimulus positioning was estimated to ~5°, which was insufficient to measure size tuning curves or delineation of receptive fields. However, all experiments involved measurement of responses to a reference stimulus (simultaneous motion in both stimulus fields) and the relative response differences between this reference condition and the test condition (motion in single stimulus field, or reduced pattern contrast). Thus the experimental design did not rely on exact positioning of the stimulus pattern.

Electrophysiology

The cells were recorded from intracellularly, using sharp glass electrodes (GC100F-10, Clark) pulled on a Brown-Flaming puller (Sutter Instruments P80-PC or P97). Their resistance when filled with 1 M KCl was 30–40 MΩ. The indifferent electrode was a wide-tip glass pipette, also used for supplying the preparation with Ringer solution. To allow focusing during an experiment, both electrode micromanipulors (Narashige), the experimental animal and the stimulus projection sphere were mounted on a common moveable platform. Neurons were penetrated in the axon by capacitance overcompensation. Voltage was amplified 10-fold (Axoclamp-2A, Axon Instruments), low-pass filtered at 2 kHz, AD-converted at an amplitude resolution of 0.244 mV per count (DT2801A, Data Translation) and stored on a computer (IBM-AT). Data were sampled at 1 kHz and stored as single traces and/or as averaged traces of 3–10 recordings. Computer programs for stimulus control, electrophysiological data acquisition, and data analysis were written in Turbo Pascal (Borland; some TP units were kindly supplied by R. Feiler, MPI für biologische Kybernetik in Tübingen, Germany). Electrical recordings were often carried out during weak tonic hyperpolarization with current injections ranging from 0.4 to 1.5 nA, i.e., during iontophoresis of the fluorescent dye. Comparison of stimulus-induced depolarizations during current injections in the mentioned range and without injection did not yield significant correlation between injected current and the amplitude or the time course of the electrical responses of the neuron.

Optical imaging

Changes in intracellular ionic calcium concentration $[Ca^{2+}]_i$ were measured as relative fluorescence changes of an intracellular calcium-sensitive dye. Typically, electrode tips were filled with a Fura-2 solution (20 mM Fura-2 pentapotassium salt, Molecular Probes; 33.3 mM KCl, 1.7 mM KOH, Merck; 29.2 mM HEPES, Sigma; pH 7.3). In some experiments with *C. stygia* a Calcium Green solution was used instead (Calcium-Green-1 hexapotassium salt, 8.7 mM, Molecular Probes; 140 mM K-acetate, Merck; 15 mM HEPES, Sigma; pH 7.3). In most cases the shaft end of the electrode was filled with Polyvinylpyrrolidon (Fluka) dissolved in 1 M KCl (Merck) to minimize dilution of the dye. After injection, the dye was left to diffuse throughout the cytoplasm for several minutes. An Hg-arc-lamp (HBO 100W, Osram; with stabilized power supply VXHC 75/100 W, Zeiss) was used for fluorescence excitation. The epifluorescence filter set for optical recording with Fura-2 consisted of a 380-nm band-pass excitation filter (bandwidth 10 nm), a 410-nm dichroic mirror and a 500- to 530-nm band-pass barrier filter. For experiments with Calcium Green the filter combination was a 472-nm excitation filter (bandwidth 17 nm), a 510-nm dichroic mirror and a 529- to 560-nm barrier filter. Image magnification was 20-fold (UD20 long-distance lens, Zeiss; numerical aperture 0.56). The focal depth was determined to be ~8–10 μm, enough for the entire dendritic arborizations of single CH or HS cells to be in focus. Fluorescence images were acquired with a Photometrics S200 camera system (16-bit Peltier-cooled charge-coupled device) driven by a Macintosh IIfx computer equipped with a NU200 controller board (Photometrics). Temporal resolution of the camera system was 0.64 Hz (128 × 128 pixel images and 200-ms exposure). In this configuration the pixel diameter was 4.5 μm. Image acquisition and processing was done by means of IPlab (Signal Analytics). During each measurement a series of 20–42 images was taken. The first exposure was used to trigger both visual stimulation and electrophysiological recording. The second image was used as the "base image" with reference to which the relative fluorescence change $\Delta F/F$ in all subsequent images of the series was calculated. To achieve higher sampling rates, single wavelength measurements were taken (excitation at λ = 380 nm). Relative fluorescence change $\Delta F/F$ is approximately proportional to $[Ca^{2+}]_i$ up to 30% (Lev-Ram et al. 1992). For tangential cells of the fly, Borst and Egelhaaf (1992) reported a resting $[Ca^{2+}]_i$ in a VS1-cell to be 50 nM. Based on this concentration, they calculated $\Delta F/F$ amplitudes of 10 and 30% to correspond to $[Ca^{2+}]_i$ increments of 34 and 135 nM, respectively. Despite the fact that Fura-2 at the used excitation wavelength exhibits fluorescence decrements in association with calcium, $\Delta F/F$ amplitudes will be inverted throughout this paper, to describe increments of $[Ca^{2+}]_i$ with positive $\Delta F/F$ values. For quantitative analyses of calcium accumulation, calculation of $\Delta F/F$ was limited to an image region, subsequently called "analyzed region." The relative fluorescence change $\Delta F/F$ was calculated for each frame of a series of images relative to a base frame, taken before stimulus presentation (for equation, see Vranesic and Knöpfel 1991). Background fluorescence was determined in an image region away from the dyed neuron. This image region remained the same for all measurements of a given cell and was chosen such that the mean background fluorescence was ~2% below the lowest fluorescence value in the analyzed region. The background fluorescence was determined separately in each frame to eliminate time-varying effects such as tissue bleaching and slight stimulus-dependent intensity changes of scattered light. For further aspects of $\Delta F/F$ calculation that are more specific to this preparation, see Dürr (1998).

A crucial aspect of $\Delta F/F$ calculation is the choice of the analyzed

region. Earlier optical-imaging studies on tangential cells (Borst and Egelhaaf 1992; Egelhaaf and Borst 1995; Egelhaaf et al. 1993) have used masks that covered only the main dendritic branches. The main argument for this restriction of the analyzed region was the exclusive visibility of the main branches, and the robust $\Delta F/F$ calculation for regions with high fluorescence compared with the ambient background. To allow consistent placement of the analyzed region in all cells, the masks used in this study covered the entire dendrite, spanning the area included by the two marginal main branches and the most distal visible fine branches. The rationale underlying this choice of the analyzed region was based on the facts that *1*) the most sensitive region within the receptive fields of HS cells is located in the frontal visual field, corresponding to the most distal zone of their dendritic arborization in the lobula plate (Hausen 1982b). Here, a given stimulus causes the largest depolarization; *2*) reconstructions of the dendrites of both cell classes have shown that their fine distal arborizations virtually cover the entire area of the lobula plate between their main dendritic branches (CH: Gauck et al. 1997; HS: Hausen 1982a; Hausen et al. 1980); *3*) even though the fine distal arborizations could not be resolved optically, the fluorescent dye diffused into those branches, causing a detectable increase in fluorescence in the regions between the visible dendritic branches and significant fluorescence changes were consistently recorded from these zones. Hence data on calcium accumulation in this paper represent spatial averages of calcium accumulation in the entire dendrite. Exceptions are the analysis of time course differences in proximal and distal branches (Fig. 3, *B* and *C*), where the original mask was divided in two parts, and the analysis of spatial overlap (Figs. 7 and 8), where the distal margin of the original mask was used to align a dorsoventral transect.

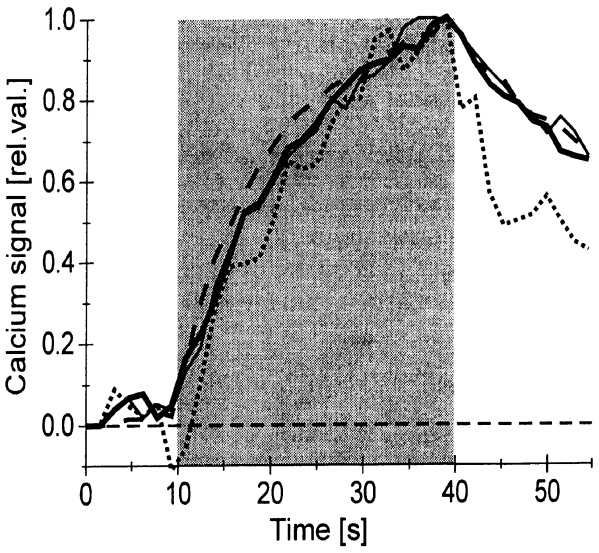

FIG. 2. Time course of calcium accumulation at different stimulus strengths. In spite of different strengths of the calcium response, the time course of accumulation remains largely invariant, as shown here for the calcium response of an HSS cell of *C. stygia*. Gray shaded area marks the 30-s stimulus period. The neuron was depolarized by 4 kinds of visual motion stimuli, differing in size, location and contrast (Size 1: thick solid line, max. $\Delta F/F$ = 34.3%, n = 3; Size 2: dotted line, max. $\Delta F/F$ = 7.5%, n = 2; Size 3: dashed line, max. $\Delta F/F$ = 45.9%, n = 2; Low Contrast: thin solid line, max. $\Delta F/F$ = 26.7%, n = 3). Stimuli of conditions Size 2 and Size 3 did not overlap in the receptive field of the neuron. After normalization with respect to their maximum, the rising phase of all response traces superimpose on each other.

RESULTS

Time course of calcium accumulation

For illustration of the correlated changes in membrane potential and $[Ca^{2+}]_i$, two representative simultaneous recordings are shown in Fig. 1. After motion onset there was a steep rise in depolarization. Due to the switched epifluorescence illumination the depolarization is superimposed by brief, large transients after each shutter opening. In HS cells, the graded depolarization showed a transient early phase, reaching a steady-state phase after a few seconds of stimulus motion. The transient onset was less pronounced in CH cells. In Fig. 1 it is followed by a sustained shallow increase of depolarization. Calcium accumulation typically resembled a low-pass filtered version of the electrical response, the rise time constant being much longer in HS cells than in CH cells. After stop of motion, depolarization decreased with comparable slope to the rising phase, overshooting into a transient afterhyperpolarization. The decay of the calcium response, on the other hand, was much slower than its rise. An after-response of reversed sign was never observed for the calcium response. In CH cells, the slope of the decreasing calcium response changes from an initial steep phase to a delayed slow decline.

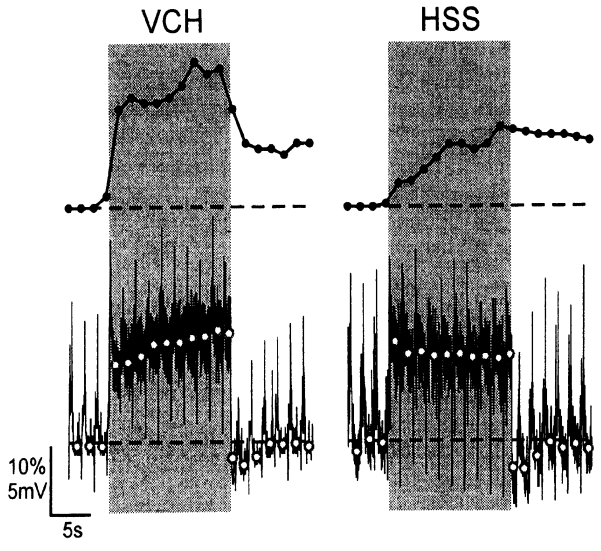

FIG. 1. Simultaneous recordings of electrical and calcium responses. *Left*: simultaneous recording of the membrane depolarization (*bottom*) and calcium accumulation (*top*, given as relative fluorescence change) of a ventral CH (VCH) cell in response to a 15-s motion stimulus (gray shaded area). Frame rate of optical recording was 0.64 Hz. To minimize bleaching, epifluorescence illumination was triggered for each camera exposure, causing brief visually induced transients in the electrical recording. To aid direct comparison of the 2 traces, the concurrent depolarization was calculated as the average membrane potential in a 900-s window, placed 500 ms after each camera exposure, thus rejecting the epifluorescence transients (open symbols). *Right*: simultaneous recordings of a Southern HS (HSS) cell. Same experimental design and graph details as above.

An interesting feature of $\Delta F/F$ time courses is their striking similarity even under very different stimulus conditions. An example is given in Fig. 2, where an HSS cell was excited by four stimuli of different size and location within the receptive field of the cell, but also of different pattern contrast. The invariance of the $\Delta F/F$ time courses became evident after normalizing each $\Delta F/F$ trace with respect to its maximum amplitude (ranging from 7.5 to 34.3% $\Delta F/F$). Although each stimulus condition was of different strength, the kinetics describing the accumulation appeared to be identical. This observation even held true when the calcium accumulation took place in different parts of the dendritic arborization, as revealed by the time courses in response to two nonoverlapping stimuli (Size 2 and Size 3 in Fig. 2).

For quantitative comparison of calcium accumulation in the

two cell classes, we mathematically described the $\Delta F/F$ time courses by the exponential function $\Delta F/F(t) = S[1 - \exp(-t/\tau)]$ (*Eq. 1*). When time constant τ and saturation level S were varied to numerically fit the average $\Delta F/F$ traces obtained from HS cells and CH cells of *C. erythrocephala*, the resulting time constant was much longer in HS cells than in CH cells at very similar saturation levels (τ = 5.3 s and τ = 1 s, respectively, Fig. 3*A*). While the HS cell response is well described by a single exponential, there is some discrepancy in case of the CH cell response, particularly after the initial 2 s of the response. Because the fast initial rise of the calcium signal in CH cells was followed by a slower sustained increase, the time course in CH cells may have been better described by two time constants. The decay time constants of the signal after stop of stimulus motion were estimated to be in the range of 10 s for CH cells and 20 s in HS cells. Fits were not calculated because time constants were longer than the measured time period. Similar to the signal increase, the course of the declining signal in CH cells suggests that it is not well described by a single time constant.

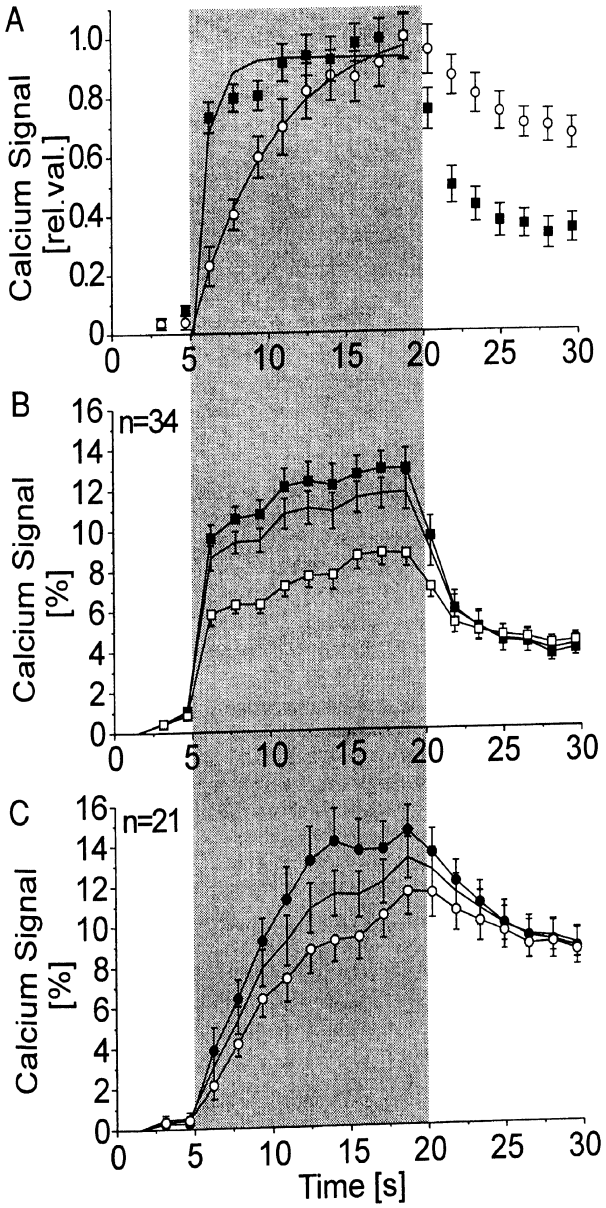

FIG. 3. Comparison of mean $\Delta F/F$ time courses for CH and HS cells. *A*: mean $\Delta F/F$ traces of 34 responses from 12 CH cells (■), 21 responses from 7 HS cells (○), normalized with respect to their maximum. Error bars denote SE. Shaded area marks the 15-s stimulus period (stimulus conditions as in Fig. 1). Solid lines show the exponential curve-fit according to *Eq. 1*. Fits were calculated to minimize errors in τ and S during the stimulus period. τ was 1 and 5.3 s, S was 11.8 and 13.2% for CH and HS cells, respectively. *B* and *C*: differences of $\Delta F/F$ time courses in thick proximal (□ and ○) and fine distal parts (■ and ●) of the dendritic arborization in CH cells (*B*) and HS cells (*C*). The proximal region was defined as the area covered by the major dendritic branches, as determined by fluorescence intensity and, thus as an electrotonically proximal region that may well extend far into the lobula plate. The distal region was defined as the remaining dendritic area. For comparison, the traces that were calculated for the entire dendritic region are included (thin lines, same as in *A*). Fits to matched pairs of distally and proximally recorded time courses yield significantly shorter time constants and lower amplitudes for CH cells than HS cells (Mann-Whitney test, τ: $P < 0.001$; S: $P < 0.05$). Distal regions exhibit significantly shorter time constants in both cell classes (Wilcoxon test: CH: $P < 0.001$; HS: $P < 0.05$) and larger amplitudes in CH cells (Wilcoxon test: CH: $P < 0.001$; HS: $P > 0.95$).

Because the branching pattern of the two cell classes differs considerably, it remained to be shown that the observed difference in kinetics of calcium accumulation was not due to the larger proportion of fine distal branches covered by the analyzed region in CH cells. Because the fine distal branches were consistently found to show the largest changes in $[Ca^{2+}]_i$, the differences found between the cell classes could well be due to differences in kinetics between distal and proximal parts of the dendritic arborization. To test the hypothesis that distal HS dendrites behave like CH dendrites, $\Delta F/F$ traces were calculated in two subregions of the original analyzed region, one covering only the thick main dendritic branches, the other covering the remaining area (Fig. 3, *B* and *C*). During stimulus motion, the mean response amplitudes in the fine dendrites were larger than the corresponding amplitudes in the main dendrites (CH: fine 12.0%, main 7.9%; HS: fine 15.5%, main 12.6%). The corresponding pairs of single recordings significantly differed in CH cells but not in HS cells. In both cell classes the time constants were significantly shorter in distal than in main dendrites (mean traces in Fig. 3, *B* and *C*, CH: fine 0.88 s, main 1.33 s HS: fine 4.77 s, main 6.71, see figure legend). Comparison between the two cell classes yielded significantly longer time constants and larger amplitudes in HS cells than in CH cells, both in fine and main dendritic branches. Thus the observed difference in calcium accumulation between the two cell classes cannot be attributed to branching pattern. Interestingly, the decay time course in main and fine branches differ only for a few seconds after stop of pattern motion, superimposing after 5–10 s.

Dependency of calcium accumulation on membrane potential

To reveal the dependency of calcium accumulation on membrane potential, it was necessary to measure the cell responses at various stimulus strengths. Egelhaaf and Borst (1995) have used pattern velocity for this purpose. However, changes in pattern velocity strongly affect the dynamic response components of tangential cells. Because the dynamic properties of the electrical responses differ between CH and HS cells, stimulus strength was altered with variable pattern contrast instead. Within the chosen range, variation of pattern contrast produced large changes in the calcium response of both cell classes, whereas the effect on membrane potential was pronounced in CH cells but not in HS cells. Figure 4 shows a representative example of this finding. Both the electrical and calcium responses of an HSS cell are displayed for three pattern contrasts.

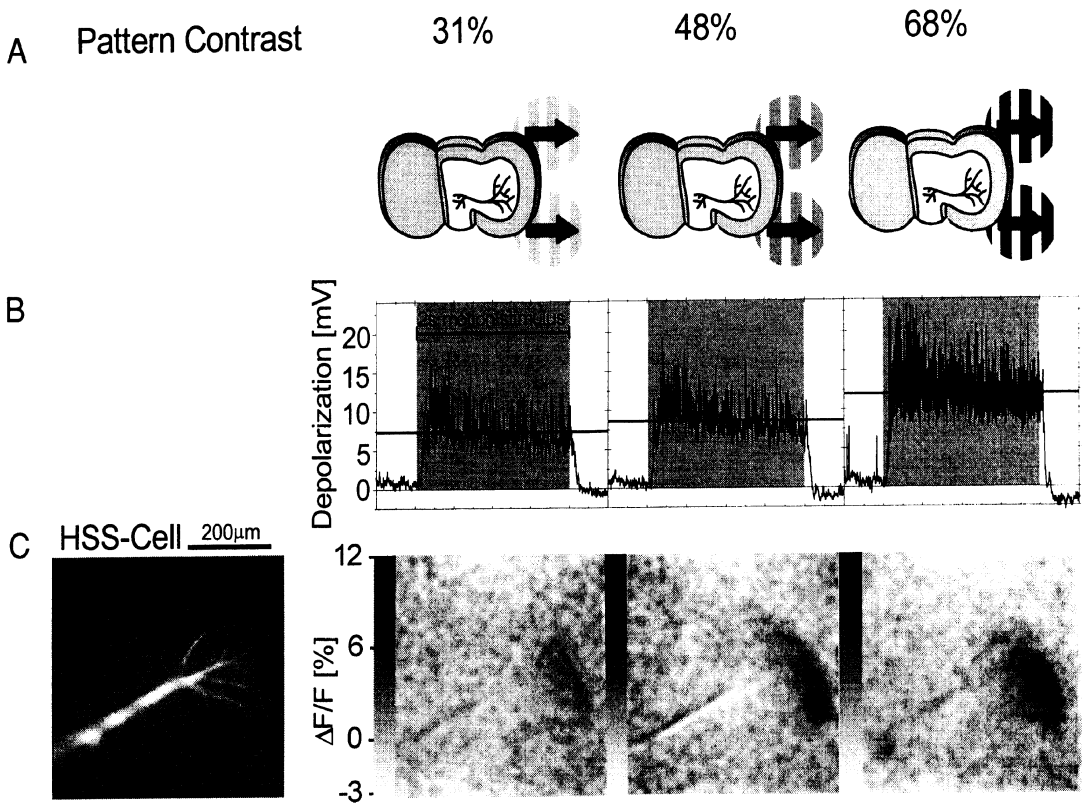

FIG. 4. Example of contrast dependency of calcium signal and membrane potential in an HSS cell. *A*: the head of a fly is viewed from behind, facing the visual stimulus, which only varied in pattern contrast. *B*: electrical responses of an HSS cell to the stimulus conditions displayed in *A*. Data are averages of 5 sweeps. The shaded area marks the stimulus period. The horizontal line is drawn at the mean depolarization level in the 1.5-s window, 400 ms after motion onset. *C*: corresponding calcium responses of the same cell. *Left image* shows the raw fluorescence image as seen through the microscope. Gray level coded images to the right show the average of 3 $\Delta F/F$ images, equivalent to the mean signal in a 4.7-s period 10 s after stimulus onset (no background subtraction; pixel values were spatially smoothed with a bell-shaped function of 5 pixels width). There is an increase from 7.3 to 12 mV (64%) in depolarization, and from 1.4 to 6.7% (479%) in the background-subtracted $\Delta F/F$ images. Note that electrophysiological and optical recordings were not acquired simultaneously and do not show the same time intervals. However, because under the given stimulus conditions the membrane depolarization was close to the steady-state response, the measured depolarization can be expected to be the same as the depolarization concurrent to the optical recording of the calcium signal.

Increase of the pattern contrast corresponded to a 64% increment of steady-state membrane depolarization and a 479% increase in the mean calcium signal. The gray-level coding of the images illustrates our common finding, that $[Ca^{2+}]_i$ increase was largest in the distal region of the dendrite, where it received input from the frontal region in visual space.

More systematic investigation of the voltage-$[Ca^{2+}]_i$ relationship revealed an almost linear dependency in CH cells but an expansive nonlinearity in HS cells (Fig. 5). After normalization with respect to the responses to the stimulus with highest contrast, the data of each cell class showed significant positive correlation between calcium signal and membrane depolarization. The qualitative observation, that HS cell data, on average, lay below the diagonal lines in Fig. 5 was statistically confirmed. In the case of HS cells, the data significantly deviated from a linear relationship, whereas the data of CH cells could not be discriminated from the linear relationship. Additionally to this statistical test, a parabolic curve fit was determined to describe the voltage-$[Ca^{2+}]_i$ relationship in each cell class. Parabolas were used for two reasons: First, the sought function needed to intersect the origin and, to account for normalization, the point (1/1). Second, the numerical procedure could be reduced to fit a single parameter (the exponent), which could be interpreted as a measure of nonlinearity. The exponent of the best-fitting parabola was 2.8 for HS cells and 1.7 for CH cells. Similar results were obtained when individual measurements were considered rather than the means of each cell.

Because the contrast dependency of the calcium accumulation was virtually the same in both cell classes (data not shown), the differing behavior of HS cells must be due to differences in the contrast dependency of electrical responses. At low pattern contrast, HS cells generally responded with larger membrane depolarization than CH cells, although the modulation range of the electrical responses was about the same in both cell classes.

Size-dependent saturation of the calcium response

When the moving pattern was presented in either one of the two stimulus fields, stimulus motion in the dorsal part of the receptive field caused a pronounced increase of $\Delta F/F$ in the dorsal branches of the dendrite, whereas ventral stimulation resulted in a pronounced increase of $\Delta F/F$ in ventral branches. Such retinotopic calcium accumulation was found in all neurons examined. Qualitatively, the local $\Delta F/F$ amplitudes in response to motion in both stimulus fields correlated well with the corresponding $\Delta F/F$ amplitudes in response to motion in two single-field responses. To quantify how well the responses to the single-field stimuli superimpose, we investigated

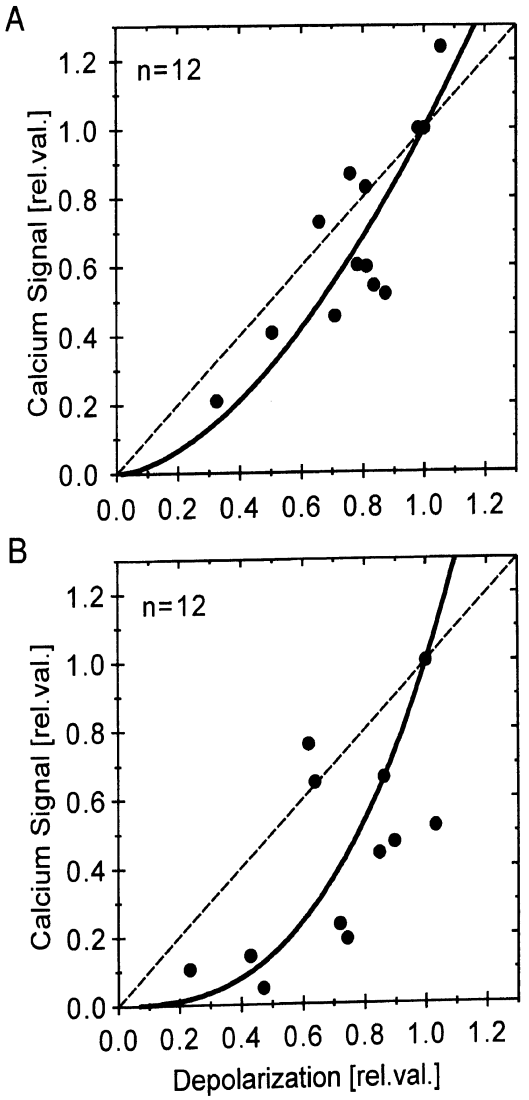

FIG. 5. Dependency of calcium accumulation on membrane potential. Mean calcium signals of 10 CH cells (*A*) and 7 HS cells (*B*) are plotted against the corresponding membrane depolarization recorded for each cell under identical stimulus conditions. The only stimulus parameter varied was pattern contrast. Mean values of each cell and stimulus condition were normalized with respect to the cell's response to the 0.68 contrast stimulus. Despite the fact that both cell classes differed in kinetics of calcium accumulation, normalization of the mean $\Delta F/F$ amplitudes rendered data of different cells immediately comparable, provided the same stimulus interval was considered in each case (Dürr 1998). Both cell classes exhibit positive correlation of calcium response and depolarization (Spearman's ranked correlation, CH: $r_S = 0.608$, $P < 0.05$, $n = 12$; HS: $r_S = 0.608$, $P < 0.05$, $n = 12$). The data significantly deviate from a linear relationship (- - - -) in HS cells, but not in CH cells (Wilcoxon test for H_0: $Y_i/X_i < 1$; CH: $P > 0.9$; HS: $P < 0.05$). Solid lines represent parabolic curve fits with exponents of 1.7 and 2.8 for CH and HS cells, respectively. The numerical procedure minimized the sum of squared *x*- and *y*-residuals of the fitted function. The resulting error function had a single minimum in both cases. Data on HS cells were pooled from *C. stygia* and *C. erythrocephala*.

whether there was size-dependent saturation of the calcium response similar to, and possibly related to the size-dependent saturation characteristic of the membrane potential (Hausen 1982b, 1984). In a second step, the spatial spread of the calcium signal was measured.

A directly comparable measure of size-dependent saturation of both response parameters was defined as the difference between the normalized linear prediction and unity: SAT = (R1 + R2)/Ref − 1 (*Eq. 2*), where the two responses to motion in either of the single stimulus fields, R1 and R2, are normalized by the reference response to simultaneous motion in both stimulus fields, Ref. The sum R1 + R2 can be interpreted as the expected response to motion in both stimulus fields in case of linear superposition. The use of a linear prediction was sensible, because the single stimulus fields did not overlap and the responses were recorded independently of each other.

Both response parameters displayed significant saturation in CH and HS cells, as denoted by positive values (Fig. 6). In other words, the increments of both response parameters became smaller the larger the size of the stimulus. Saturation of the calcium and electrical responses could not be statistically discriminated in CH cells, but they marginally differed in HS cells, corroborating the previous finding of a nonlinear voltage-$[Ca^{2+}]_i$ relationship in HS cells, when stimulus contrast was varied rather than size. Comparison of the same response parameters between CH and HS cells revealed a significant difference in the saturation of the membrane potential but not in the saturation of the calcium signal.

Overlapping calcium signals in response to nonoverlapping stimuli

In spite of the general validity of the observation that calcium accumulation is a retinotopic process, it was evident that there was considerable spatial overlap of the calcium responses to nonoverlapping stimuli. The area and amplitude of spatially overlapping calcium signals in response to nonoverlapping stimuli were determined from the same experiments as those performed to investigate the size dependency. Given the retinotopic columnar structure of the optic lobes (Strausfeld 1976), excitation of two spatially disjunct areas of the retina will lead to excitation of different populations of input elements to the lobula plate. Because the exact border of the dendritic region that actually received synaptic input cannot be determined, the

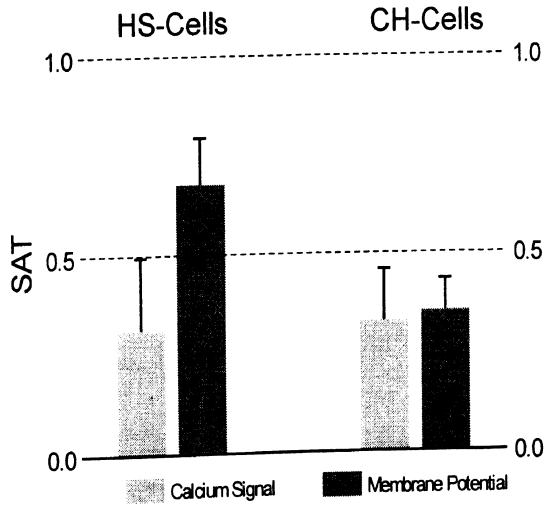

FIG. 6. Saturation of calcium accumulation with increasing stimulus size. Saturation characteristics, SAT, for CH and HS cells (mean ± SE) reveal size-dependent saturation in both cell classes and both response parameters (Wilcoxon test for H_0: SAT > 0; CH: $P < 0.01$ for calcium; $P < 0.005$ for depolarization, $n = 12$; HS: $P < 0.05$ for calcium, $P < 0.01$ for depolarization, $n = 9$). SAT in CH and HS cells differ with respect to depolarization but not with respect to calcium accumulation (Mann-Whitney test for H_0: HS > CH; depolarization: $P < 0.05$; calcium: $P > 0.5$). SAT in depolarization and calcium signal differ marginally in HS cells but not in CH cells (Wilcoxon test for H_0: Dep > Ca; HS: $P < 0.1$; CH: $P > 0.75$). Data on HS cells were pooled from *C. stygia* and *C. erythrocephala*.

spatial spread of the signal was quantified by relating the two single-field responses (Fig. 7).To do so, a topographic map of the overlapping signal was calculated from two corresponding $\Delta F/F$ images. Each pixel contained the smaller one of the two $\Delta F/F$ amplitudes that were recorded at this location in response to either stimulus field (Fig. 7*D*). Two parameters were quantified to describe the overlapping signal: area and amplitude profile.

The area of overlap was quantified for a given threshold $\Delta F/F$ amplitude. To make the threshold comparable between different cells, it was expressed as a fraction of the maximum amplitude recorded in response to simultaneous motion in both stimulus fields. Because the choice of a particular threshold was arbitrary, this procedure was repeated for a range of four thresholds. Obviously, the area of overlap was smaller, the higher the threshold (Fig. 8*A*). The area of overlap largely scaled with the size of the dendritic tree. Thus in spite of the much larger arborizations in CH cells than in HS cells, the relative area remained comparable, although the mean values of CH cells were consistently larger than those of HS cells, irrespective of the chosen threshold. At a threshold of 50% of the maximum response, the area of overlap was close to zero in both cell classes.

Quantification of the amplitude profile across the dendrite was carried out for six VCH cells and six HS cells (Fig. 8*B*). In these cells, the local $\Delta F/F$ amplitudes were determined along a vertical transect across the distal part of the dendrite. This was done by calculation of the mean $\Delta F/F$ amplitudes in horizontal pixel lines, equivalent to a 90-μm-wide stripe across the distal lobula plate, corresponding to the input zone of the frontal visual field (Strausfeld 1976). An example of a single overlap profile is shown in Fig. 7*D*. Because the exact midline between the excited input regions on the dendrite could not be determined, comparison of individual profiles required them to be centered with respect to their maximum. The average overlap profiles are given in Fig. 8*B*. Because, on average, HS cells exhibited stronger calcium accumulation than CH cells, normalization resulted in further separation of the overlap profiles in VCH and HS cell. The amplitude of overlap in VCH cells reached the mean response level in this region and was about twice as large as in HS cells. Similar results were obtained for an earlier time window (1st 4.6 s, data not shown), indicating that the spatial extent of the overlap does not greatly vary in time.

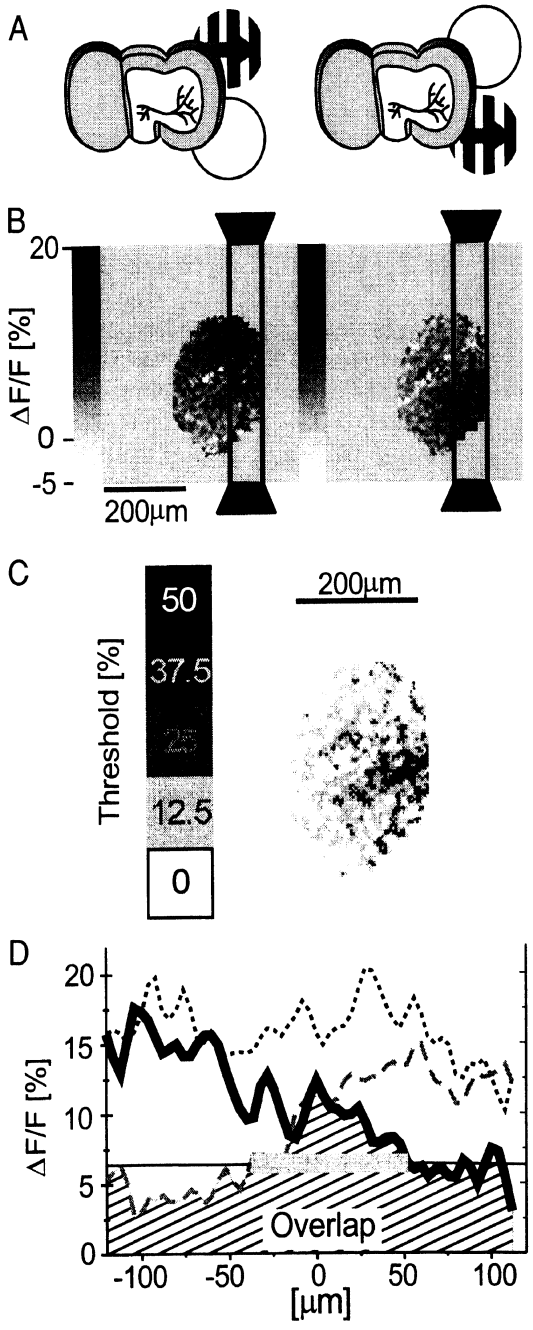

FIG. 7. Measuring spatial overlap of calcium signals in response to nonoverlapping stimuli. *A*: the head of a fly is viewed from behind, facing the visual stimulus. Two nonoverlapping stimuli excited spatially disjunct regions of the retina. Separation of the stimuli was ~3°. *B*: calcium responses to the stimulus conditions in a VCH cell. The oval analyzed region covers only the dendritic arborization of the VCH cell, i.e., all pixels outside this region were set to zero. Darker pixels indicate larger $\Delta F/F$ amplitudes. The vertical bands limit the transect, along which the amplitude profile of the overlap was determined. The distal margin of the transect coincided with the margin of the analyzed region. *C*: topographic map of the overlapping signal. Each pixel was assigned the gray level of the highest threshold it surpassed. Darker gray levels indicate higher threshold $\Delta F/F$ amplitudes. Thresholds were chosen relative to the maximum $\Delta F/F$ amplitude in response to motion in both stimulus fields. *D*: amplitude profile of the overlap along the vertical transects shown in the left image in *B* (thick solid line, dorsal stimulation) and the right image in *B* (thick broken line: ventral stimulation). The 3rd profile refers to the response to simultaneous motion in both stimulus fields is included (thin dashed line). $\Delta F/F$ thresholds for the quantification of the area of overlap were chosen with respect to the maximum of this transect. The local amplitude of the overlap profile was defined as the smaller $\Delta F/F$ amplitude of the 2 responses at a given location (hatched area). Profile amplitudes were calculated for each horizontal pixel line (15–30 pixels). The analysis was run with respect to the horizontal borders of the image. To compensate for the angle of the cell midline against the horizontal, the width of the transect had to be chosen for each cell such that an average of 20 pixels and at least 15 pixels per line were considered.

DISCUSSION

Visual motion stimuli induced calcium accumulation in combined pre- and postsynaptic CH cell dendrites and purely postsynaptic HS cell dendrites. Dendritic calcium accumulation followed an invariant time course in both cell classes with time constants being shorter in CH cells than in HS cells. In both cell classes, calcium accumulation was stronger in fine distal branches than in thick proximal branches. The relationship of calcium accumulation and concurrent membrane potential differed considerably between types of dendrite. Both cell classes exhibited size-dependent saturation of the calcium

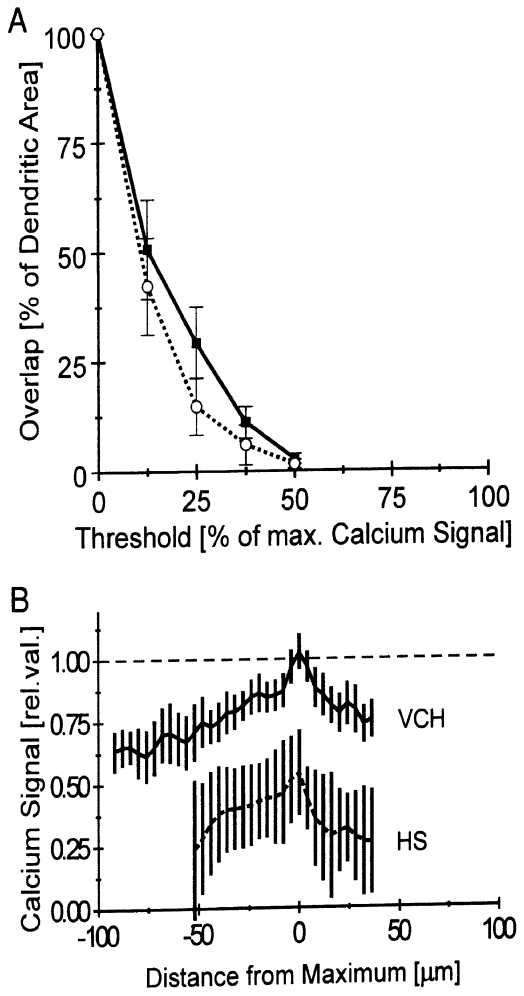

FIG. 8. Area and amplitude of the overlapping signal. *A*: dependency of the overlap measure on the $\Delta F/F$ threshold. Traces were normalized with respect to their maximum, i.e., the average area of the dendritic arborization in the lobula plate. Thus the plotted values are equivalent to the percentage of pixels in the analyzed region the values of which lay above the threshold. The threshold is expressed as a fraction of the maximum $\Delta F/F$ amplitude recorded in response to simultaneous motion in both stimulus fields. Error bars denote SE. The total area of overlap was consistently larger in CH cells (■, n = 12), than in HS cells (○, n = 9). The area of overlap approximately scales to the total area of the dendritic arborization. *B*: amplitude profiles of overlap along a vertical transect through the distal area of the lobula plate (mean ± SE). Six VCH (—) and 6 HS cells (3 HSE and HSS each, - - -) in the 4.6-s period 10 s after motion onset (equivalent to 4 camera exposures, same interval as in *A*). Before averaging, individual traces were shifted with respect to their peak amplitude. Therefore the given distances are relative measures and do not correspond to any fixed point in the lobula plate. Traces are shown for the range in which at least 5 values were available and normalized with respect to the mean amplitude in the reference profile. The latter was determined during motion in both stimulus fields (CH: 14.8%; HS: 18.7%.).

response. The spatial spread of the calcium signal was investigated by evaluating the spatial overlap of the calcium responses to spatially nonoverlapping stimuli. Both the amplitude and the area of overlap of the calcium signal were larger in CH than in HS cells, indicating a larger extent of blurring of the retinotopic input pattern across the CH dendrite compared with the HS dendrite.

Time course of calcium accumulation and decay

The major entry mode of calcium ions into the cytoplasm can be considered a voltage-dependent calcium influx via the cell membrane. Voltage-dependent calcium accumulation has been reported for several kinds of tangential cells in vivo (Egelhaaf and Borst 1995; Single and Borst 1997, 1998) and in vitro (Oertner and Borst 1997). To date, a cobalt-blockable calcium current has only been shown for CH cells (Haag et al. 1997). Because, in principle, voltage-dependent calcium accumulation could also arise from electrogenic Na/Ca exchangers in the cell membrane (Blaustein 1988; Kostyuk 1992), experimental evidence for the existence of voltage-dependent calcium channels is still required for HS cells. Calcium entry via cholinergic ligand-gated ion channels may contribute to some extent (Oertner and Borst 1997) but must be expected to be negligible compared with voltage-dependent calcium influx, because null direction motion does not induce large changes in HS cells (Egelhaaf and Borst 1995), although cholinergic ion channels are thought to be active also during null direction motion (Borst et al. 1995; Single et al. 1997). Recently claimed calcium decrease during null direction motion in all tangential cells of the lobula plate (Single and Borst 1998) was found in our own experiments only in case of CH cells but not in HS cells (Dürr, Kurtz, and Egelhaaf, unpublished observations). The latter difference may cause the faster decline of $[Ca^{2+}]_i$ in CH cells than in HS cells during poststimulus afterhyperpolarization.

Both the invariance of the time course and the dependency of the maximum $[Ca^{2+}]_i$ on stimulus parameters are in accordance with an analytic model of residual intracellular calcium dynamics by Tank et al. (1995). Although their model predicts the rise and decay kinetics of $[Ca^{2+}]_i$ to be strongly dependent on the concentration of intracellular calcium buffers, the plateau concentration is expected to remain unaffected by these buffers. Rather, the maximum $[Ca^{2+}]_i$ is determined by the equilibrium of calcium influx and extrusion across the cell membrane. Applying this model to the dendrites under investigation, the similar $\Delta F/F$ amplitudes observed in CH and HS cells suggest a similar balance of calcium entry and extrusion in each of both cell classes. Moreover, the considerable differences between the kinetics of the calcium response in CH and HS cells may be due to different native buffer systems. In principle, a systematic difference in the Fura-2 concentration in both cell classes, e.g., due to a larger cytoplasm volume in CH cells, could mimic the same effect. However, because fluorescence in branches of comparable diameter in both cell classes did not vary systematically, a biasing effect due to dye concentration should be negligible. The single time constant describing the calcium accumulation in HS cells (Fig. 3*A*) suggests that a single cellular mechanism is dominating the dynamics of the calcium signal.

Although the simple model by Tank et al. (1995) plausibly describes accumulation of residual calcium in tangetial cells, other mechanisms, not included in this model, possibly contribute their share to the time course of neuronal $[Ca^{2+}]_i$. For instance, in spite of limited intracellular diffusion of calcium ions in neurons (Gabso et al. 1997) mobile buffers can greatly enhance intracellular diffusability (Zhou and Neher 1993). Furthermore, sequestration of calcium ions in mitochondria as well as in the endoplasmatic reticulum is known to be effective in neurons on a short time scale (Markram et al. 1995; Pivovarova et al. 1997; Pozzo-Miller et al. 1997).

Voltage dependency and spatial overlap

Variation of stimulus strength by means of pattern contrast revealed an expansive nonlinearity of the voltage-$[Ca^{2+}]_i$ relationship in HS cells (Fig. 4). This suggests the presence of a voltage threshold for calcium entry into the cell. Because in CH cells this relationship did not significantly deviate from linearity, a possible voltage threshold of calcium entry in CH cells is expected to be lower than in HS cells. Different thresholds of calcium entry in CH and HS cells are likely to reflect different kinds of voltage-gated calcium channels in the dendrites of CH and HS cells. In spite of the qualitative finding of local calcium accumulation in CH and HS cells (Borst and Egelhaaf 1992; Egelhaaf and Borst 1995; Egelhaaf et al. 1993; Single and Borst 1998) and the availability of detailed compartmental models of the intrinsic properties of these cells (Borst and Haag 1996; Haag et al. 1997), very little is known about the link between membrane potential and spatial spread of $[Ca^{2+}]_i$.

Both cell classes reveal size-dependent saturation of both calcium accumulation and membrane depolarization (Fig. 6). While the size-dependent saturation of the calcium signal in CH cells paralleled the saturation observed for the electrical response, such matching did not exist in HS cells. This corroborates our measurements of contrast dependency. Size-dependent saturation of the membrane depolarization has been reported earlier for HS cells (Hausen 1982b) and CH cells (Egelhaaf et al. 1994). The latter results also suggested considerable spatial spread of motion-induced depolarization in the dendritic arborization of CH cells, quite contrary to what would be expected from their passive membrane properties (Borst and Haag 1996).

Whereas we found a saturation nonlinearity in size-dependent calcium accumulation in the CH cells, a size-dependent expansive nonlinearity was postulated in a previous study (Egelhaaf et al. 1993). While the conclusions drawn in the present study are based on quantitative analysis of calcium accumulation in a sufficiently large sample of CH cells and could be tested statistically, this was not the case in the earlier study, where the conclusions drawn with respect to calcium accumulation were solely derived from qualitative evidence. As a consequence, the current hypothesis of small-field tuning in certain tangential cells (Borst and Egelhaaf 1993) will have to be refined.

Because the spatial divergence of retinotopic columnar processing has never been examined on a comparably small range, it cannot be ruled out that the observed overlap is due to presynaptic divergence of the input, rather than due to postsynaptic expansion of the depolarization. Yet, because several lines of evidence (see *Comparison of purely postsynaptic dendrites with pre- and postsynaptic dendrites*) indicate similar retinotopic input to CH and HS cells, divergence of the retinotopic input, if present, should result in similar overlap of the calcium signal in both cell classes. According to Hausen (1981), divergence of the excitation pattern to CH cells could be caused by nonretinotopic, recurrent excitation of the CH cell via the two heterolateral H1 cells and the contralateral CH cells. Although this scenario requires a succession of activity changes across four synaptic interfaces, the effect of which seems debatable, it needs to be tested in further experiments using microsurgical lesions of the heterolateral pathways (e.g., Hausen and Wehrhahn 1990). More pronounced diffusion in the spread of calcium in VCH than in HS cells is unlikely for the following reasons. *1*) The dense branching pattern of CH cells does not support fast diffusion due to short distances. *2*) Significantly enhanced diffusion in CH cells would require raised concentration of mobile calcium buffers (see *Time course of calcium accumulation and decay*). This, however, is in conflict with the finding of the short time constant, which should rather be prolonged by high buffer concentrations (Tank et al. 1995).

Voltage-dependent calcium influx must be dependent on the spatial spread of the postsynaptic depolarization, but also on the activation properties of the voltage-dependent process underlying the influx. Compartmental-model simulations of the active properties in HS cells suggest that "HS cells become significantly less compact [than expected from the passive membrane properties] during depolarization due to the increased potassium conductance" (Haag et al. 1997, p. 363). Both the high-threshold activation of calcium entry that was suggested above and the reduced compactness during depolarization are active membrane properties favoring highly local dendritic calcium accumulation in HS cells. On the other hand, the absence of either of these two active mechanisms in CH cells is in agreement with spatial blurring of the calcium signal in CH cells.

Comparison of purely postsynaptic dendrites with pre- and postsynaptic dendrites

The observed differences of motion-induced calcium accumulation in CH and HS cells are summarized in Table 1. Although there is a number of anatomically known input elements to the lobula plate (Douglass and Strausfeld 1995, 1996, 1998; Strausfeld 1976), the physiological identity of the input to CH and HS cells is still a matter of speculation. Yet, there are several lines of evidence supporting the view that CH and HS cells receive similar ipsilateral input. *1*) The arboriza-

TABLE 1. *Comparison of calcium accumulation in centrifugal horizontal and horizontal system cells in response to ipsilateral motion*

	CH Cells	HS Cells
Computational function	Relay of input activation pattern within the lobula plate	Extraction of yaw rotation/output to descending neurons
Behavioral context	Figure-ground segregation	Horizontal optomotor turning response
Rise time constant	≈1 s	≈5–6 s
Decay time constant	≈10 s	≈20 s
Maximum amplitude of $\Delta F/F^*$	11.8 ± 0.86%	13.2 ± 1.02%
Size dependency	Saturation nonlinearity, similar to electrical response	Saturation nonlinearity, different from electrical response
Voltage-$[Ca^{2+}]_i$ relationship	Approximately linear/low threshold	Expansive nonlinearity/high threshold
Spatial overlap	Strong	Moderate

Values in Maximum amplitude of $\Delta F/F$ are means ± SE after 15 s of motion (contrast: 68%; temporal frequency: 2 Hz; λ = 33°; luminance: 230 cd/m^2).

tions of the two CH and the three HS cells cover the same area in the lobula plate (Eckert and Dvorak 1983; Hausen 1982a) and are located in close vicinity (Strausfeld et al. 1995, their Fig. 2). *2*) In their ipsilateral receptive field, both cell classes share the same directional selectivity, both on a global (Gauck et al. 1997; Hausen 1982b) and on a local scale (H. Krapp, personal communication). *3*) Retinotopic calcium acccumulation in both cell classes indicates retinotopic input from local small field elements (Egelhaaf et al. 1993; Egelhaaf and Borst 1995). An earlier hypothesis (e.g., Hausen 1984) according to which HS cells give ipsilateral input to CH cells could be ruled out because only a contralateral motion stimulus causes calcium accumulation in the putative HS-CH input region (Egelhaaf et al. 1993, Fig. 4). *4*) Finally, detailed analysis of the local motion detector inputs yielded similar results for both cell classes (Kondoh et al. 1995).

Because the neuronal substrate underlying the similar input is still unknown, further experiments are needed to tell intrinsic from extrinsic contributions to the described differences. If synaptic input to CH and HS cells were the same, the described differences in calcium accumulation would be determined entirely by the biophysical properties of the dendrites. An alternative explanation would be that CH and HS cells pool information from different sets of input elements, or at least differ in the number and distribution of their postsynaptic sites.

The computational task of CH cells is to relay retinotopic information within the lobula plate via inhibitory dendritic synapses. The presented spatiotemporal properties of calcium accumulation in CH cells imply that postsynaptic neurons to CH cells, such as the FD1 cell (Warzecha et al. 1993), receive a spatially low-pass filtered inhibitory signal acting with a time constant no longer than 1 s. It is a plausible assumption that dendritic intracellular calcium in CH cells causes transmitter release in their presynaptic terminals. However, the extent to which the measured calcium accumulation actually reflects the activation of synaptic transmitter release is yet to be demonstrated. In HS cells, dendritic intracellular calcium has only postsynaptic functions as a charge carrier and possible modulatory roles on membrane proteins, including ion channels. Here, calcium accumulation is more than five times slower than in CH cells and remains locally confined for time periods of several seconds. Because of these characteristics, it has been suggested that a possible modulatory role of intracellular calcium in HS cells may be in motion adaptation (Dürr and Egelhaaf 1998). Of course, the same modulatory role cannot be excluded to exist in CH cells too, yet the different voltage-$[Ca^{2+}]_i$ relationships between both cell classes should lead to marked differences in the voltage dependency of any modulatory mechanism and thus offers a set of testable predictions.

Because dendrodendritic synapses are a common feature of vertebrate and invertebrate nervous systems, e.g., in the retina and olfactory bulb of vertebrates (Nakanishi 1995) or in stomatogastric and thoracic ganglia of arthropods (Graubard 1978; Laurent 1993), the described fast low-pass–filtered relaying of an excitation pattern may prove to be a common computational feature of this synaptic design.

We thank R. Kurtz and A.-K. Warzecha for helpful comments on the manuscript.

This work was supported by a grant from the Deutsche Forschungsgemeinschaft (DFG).

Present address and address for reprint requests: V. Dürr, Abteilung Biokybernetik und Theoretische Biologie, Fakultät für Biologie, Universität Bielefeld, Postfach 10 01 31, D-33501 Bielefeld, Germany.

Received 19 March 1999; accepted in final form 6 August 1999.

REFERENCES

BERRIDGE, M. J. Elementary and global aspects of calcium signalling. *J. Physiol. (Lond.)* 499: 291–306, 1997.

BLAUSTEIN, M. P. Calcium transport and buffering in neurons. *Trends Neurosci.* 11: 438–443, 1988.

BORST, A. AND EGELHAAF, M. In vivo imaging of calcium accumulation in fly interneurons as elicited by visual motion stimulation. *Proc. Natl. Acad. Sci. USA* 89: 4139–4143, 1992.

BORST, A. AND EGELHAAF, M. Processing of synaptic signals in fly visual interneurons selectively responsive to small moving objects. In: *Brain Theory,* edited by A. Aertsen. New York: Elsevier, 1993, p. 47–66.

BORST, A. AND EGELHAAF, M. Dendritic processing of synaptic information by sensory interneurons. *Trends Neurosci.* 17: 257–263, 1994.

BORST, A., EGELHAAF, M., AND HAAG, J. Mechanisms of dendritic integration underlying gain control in fly motion-sensitive interneurons. *J. Comput. Neurosci.* 2: 5–18, 1995.

BORST, A. AND HAAG, J. The intrinsic electrophysiological characteristics of fly lobula plate tangential cells. I. Passive membrane properties. *J. Comput. Neurosci.* 3: 313–336, 1996.

DENK, W., YUSTE, R., SVOBODA, K., AND TANK, D. W. Imaging calcium dynamics in dendritic spines. *Curr. Opin. Neurobiol.* 6: 372–378, 1996.

DOUGLASS, J. K. AND STRAUSFELD, N. J. Visual motion detection circuits in flies: peripheral motion computation by identified small-field retinotopic neurons. *J. Neurosci.* 15: 5596–5611, 1995.

DOUGLASS, J. K. AND STRAUSFELD, N. J. Visual motion-detection circuits in flies: parallel direction- and non–direction-sensitive pathways between the medulla and lobula plate. *J. Neurosci.* 16: 4551–4562, 1996.

DOUGLASS, J. K. AND STRAUSFELD, N. J. Functionally and anatomically segregated visual pathways in the lobula complex of a calliphorid fly. *J. Comp. Neurol.* 396: 84–104, 1998.

DÜRR, V. *Dendritic Calcium Accumulation in Visual Interneurons of the Blowfly* (PhD dissertation). Bielefeld, Germany: Univ. of Bielefeld, 1998.

DÜRR, V. AND EGELHAAF, M. Dendritic calcium accumulation in visual interneurons of *Calliphora*. Dependence on stimulus size and contrast. *Proc. Göttingen Neurobiol. Conf.* 25: 489, 1997.

DÜRR, V. AND EGELHAAF, M. Is there a dendritic mechanism underlying visual motion adaptation? *Proc. Göttingen Neurobiol. Conf.* 26: 133, 1998.

ECKERT, H. AND DVORAK, D. R. The centrifugal horizontal cells in the lobula plate of the blowfly, *Phaenicia sericata*. *J. Insect Physiol.* 29: 547–560, 1983.

EGELHAAF, M. On the neuronal basis of figure-ground discrimination by relative motion in the visual system of the fly. II. Figure-detection cells, a new class of visual interneurons. *Biol. Cybern.* 52: 195–209, 1985.

EGELHAAF, M. AND BORST, A. A look into the cockpit of the fly: visual orientation, algorithms, and identified neurons. *J. Neurosci.* 13: 4563–4574, 1993.

EGELHAAF, M. AND BORST, A. Calcium accumulation in visual interneurons of the fly: stimulus dependency and relationship to membrane potential. *J. Neurophysiol.* 73: 2540–2552, 1995.

EGELHAAF, M., BORST, A., WARZECHA, A.-K., FLECKS, S., AND WILDEMANN, A. Neural circuit tuning fly visual interneurons to motion of small objects. II. Input organization of inhibitory circuit elements revealed by electrophysiological and optical recording techniques. *J. Neurophysiol.* 69: 340–351, 1993.

EGELHAAF, M., HAAG, J., AND BORST, A. Processing of synaptic information depends on the structure of the dendritic tree. *NeuroReport* 6: 205–208, 1994.

GABSO, M., NEHER, E., AND SPIRA, M. E. Low mobility of the Ca^{2+}-buffers in axons of cultured *Aplysia* neurons. *Neuron* 18: 473–481, 1997.

GAUCK, V., EGELHAAF, M., AND BORST, A. Synapse distribution on VCH, an inhibitory, motion-sensitive interneuron in the fly visual system. *J. Comp. Neurol.* 381: 489–499, 1997.

GEIGER, G. AND NÄSSEL, D. R. Visual orientation behavior of flies after selective laser beam ablation of interneurons. *Nature* 293: 398–399, 1981.

GEIGER, G. AND NÄSSEL, D. R. Visual processing of moving single objects and wide-field patterns in flies: behavioral analysis after laser-surgical removal of interneurons. *Biol. Cybern.* 44: 141–149, 1982.

GHOSH, A. AND GREENBERG, M. E. Calcium signalling in neurons: molecular mechanisms and cellular consequences. *Science* 268: 239–247, 1995.

GRAUBARD, K. Synaptic transmission without action potentials: Input-output properties of a non-spiking presynaptic neuron. *J. Neurophysiol.* 41: 1014–1025, 1978.

HAAG, J. AND BORST, A. Amplification of high-frequency synaptic inputs by active dendritic membrane processes. *Nature* 379: 639–641, 1996.

HAAG, J., THEUNISSEN, F., AND BORST, A. The intrinsic electrophysiological characteristics of fly lobula plate tangential cells. II. Active membrane properties. *J. Comput. Neurosci.* 4: 349–369, 1997.

HARDIE, R. C. Functional organization of the fly retina. *Prog. Sensory Physiol.* 5: 1–80, 1982.

HARDIE, R. C. Calcium signalling: setting store by calcium channels. *Curr. Biol.* 6: 1371–1373, 1996.

HAUSEN, K. Functional characterization and anatomical identification of motion sensitive neurons in the lobula plate of the blowfly *Calliphora erythrocephala*. *Z. Naturforsch.* 31: 629–633, 1976.

HAUSEN, K. Monocular and binocular computation of motion in the lobula plate of the fly. *Verh. Dt. Zool. Ges.* 1981: 49–70, 1981.

HAUSEN, K. Motion sensitive interneurons in the optomotor system of the fly. I. The horizontal cells: structure and signals. *Biol. Cybern.* 45: 143–156, 1982a.

HAUSEN, K. Motion sensitive interneurons in the optomotor system of the fly. II. The horizontal cells: receptive field organization and response characteristics. *Biol. Cybern.* 46: 67–79, 1982b.

HAUSEN, K. The lobula-complex of the fly: structure, function and significance in visual behavior. In: *Photoreception and Vision in Invertebrates,* edited by M. A. Ali. New York: Plenum, 1984, p. 523–555.

HAUSEN, K. AND EGELHAAF, M. Neural mechanisms of visual course control in insects. In: *Facets of Vision,* edited by D. G. Stavenga and R. C. Hardie. Berlin: Springer, 1989, p. 391–424.

HAUSEN, K. AND WEHRHAHN, C. Neural circuits mediating visual flight control in flies. I. quantitative comparison of neural and behavioral response characteristics. *J. Neurosci.* 9: 3828–3836, 1989.

HAUSEN, K. AND WEHRHAHN, C. Neural Circuits mediating visual flight control in flies. II. Separation of two control systems by microsurgical brain lesions. *J. Neurosci.* 10: 351–360, 1990.

HAUSEN, K., WOLBURG-BUCHHOLZ, K., AND RIBI, W. A. The synaptic organization of visual interneurons in the lobula complex of flies. *Cell Tissue Res.* 208: 371–387, 1980.

HEISENBERG, M., WONNEBERGER, R., AND WOLF, R. Optomotor-blind H31—a *Drosophila* mutant of the lobula plate giant neurons. *J. Comp. Physiol. [A]* 124: 287–296, 1978.

KATZ, B. *The Release of Neural Transmitter Substances.* Springfield, IL: Thomas, 1969.

KONDOH, Y., HASEGAWA, Y., OKUMA, J., AND TAKAHASHI, F. Neural computation of motion in the fly visual system: quadratic nonlinearity of responses induced by picrotoxin in the HS and CH cells. *J. Neurophysiol.* 74: 2665–2684, 1995.

KOSTYUK, P. G. *Calcium Ions in Nerve Cell Function.* New York: Oxford Univ. Press, 1992

LAURENT, G. A dendritic gain control mechanism in axonless neurons of the locust, *Schistocerca americana*. *J. Physiol. (Lond.)* 470: 45–54, 1993.

LEV-RAM, V., MIYAKAWA, H., LASSER-ROSS, N., AND ROSS, W. N. Calcium transients in cerebellar purkinje neurons evoked by intracellular stimulation. *J. Neurophysiol.* 68: 1167–1177, 1992.

MARKRAM, H., HELM, P. J., AND SAKMANN, B. Dendritic calcium transients evoked by single back-propagating action potentials in rat neocortical pyramidal neurons. *J. Physiol. (Lond.)* 485: 1–20, 1995.

MEYER, E. P., MATUTE, C., STREIT, P., AND NÄSSEL, D. R. Insect optic lobe neurons identifiable with monoclonal antibodies to GABA. *Histochemistry* 84: 207–216, 1986.

NAKANISHI, S. Second-order neurones and receptor mechanisms in visual and olfactory information processing. *Trends Neurosci.* 18: 359–364, 1995.

OERTNER, T. G. AND BORST, A. Mechanisms of calcium entry in visual interneurons of the blowfly. *Soc. Neurosci. Abstr.* 23: 262.10, 1997.

OGAWA, H., BABA, Y., AND OKA, K. Dendritic Ca^{2+} response in cercal sensory interneurons of the cricket *Gryllus bimaculatus*. *Neurosci. Lett.* 219: 21–24, 1996.

PIVOVAROVA, N. B., POZZO-MILLER, L. D., LEAPMAN, R. D., O'CONNELL, M. F., REESE, T. S., AND ANDREWS, S. B. Rapid calcium accumulation by endoplasmatic eticulum and mitochondria after synaptic activation of CA3 pyramidal dendrites in hippocampal slices. *Soc. Neurosci. Abstr.* 23: 1127, 1997.

POZZO-MILLER, L. D., PIVOVAROVA, N. B., LEAPMAN, R. D., BUCHANAN, R. A., REESE, T. S., AND ANDREWS, S. B. Activity-dependent calcium sequestration in dendrites of hippocampal neurons in brain slices. *J. Neurosci.* 17: 8729–8738, 1997.

REGEHR, W. G. AND TANK, D. W. Dendritic calcium dynamics. *Curr. Opin. Neurobiol.* 4: 373–382, 1994.

SAH, P. Ca-activated K currents in neurones: types, physiological roles and modulation. *Trends Neurosci.* 19: 150–155, 1996.

SINGLE, S. AND BORST, A. In vivo measurements of calcium dynamics in visual interneurons. *Soc. Neurosci. Abstr.* 23: 262.9, 1997.

SINGLE, S. AND BORST, A. Dendritic integration and its role in computing image velocity. *Science* 281: 1848–1850, 1998.

SINGLE, S., HAAG, J., AND BORST, A. Dendritic computation of direction selectivity and gain control in visual interneurons. *J. Neurosci.* 17: 6023–6030, 1997.

SKEER, J. M., NORMAN, R. I., AND SATTELLE, D. B. Invertebrate voltage-dependent calcium channel subtypes. *Biol. Rev.* 71: 137–154, 1996.

SOBEL, E. C. AND TANK, D. W. In vivo calcium dynamics in a cricket auditory neuron: an example of chemical computation. *Science* 263: 823–827, 1994.

STRAUSFELD, N. J. *Atlas of an Insect Brain.* Berlin: Springer, 1976.

STRAUSFELD, N. J., KONG, A., MILDE, J. J., GILBERT, C., AND RAMAIAH, L. Oculomotor control in calliphorid flies: GABAeergic organization in heterolateral inhibitory pathways. *J. Comp. Neurol.* 361: 298–320, 1995.

SVOBODA, K., DENK, W., KLEINFELD, D., AND TANK, D. W. In vivo dendritic calcium dynamics in neocortical pyramidal neurons. *Nature* 385: 161–165, 1997.

TANK, D. W., REGEHR, W. G., AND DELANEY, K. R. A quantitative analysis of presynaptic calcium dynamics that contribute to short-term enhancement. *J. Neurosci.* 15: 7940–7952, 1995.

VRANESIC, I. AND KNÖPFEL, T. Calculation of calcium dynamics from single wavelength fura-2 fluorescence recordings. *Pflügers Arch.* 418: 184–189, 1991.

WARZECHA, A.-K., EGELHAAF, M., AND BORST, A. Neural circuit tuning fly visual interneurons to motion of small objects. I. Dissection of the circuit by pharmacological and photoinactivation techniques. *J Neurophysiol.* 69: 329–339, 1993.

ZHOU, Z. AND NEHER, E. Mobile and immobile calcium buffers in bovine adrenal chromaffine cells. *J. Physiol. (Lond.)* 469: 245–273, 1993.